^{1}H-NMR-based metabolic profiling of a colorectal cancer CT-26 lung metastasis model in mice

YAN LI[1*], CHUNTING WANG[1*], DANDAN LI[1*], PENGCHI DENG[2], XIAONI SHAO[1], JING HU[1], CHUNQI LIU[1], HUI JIE[1], YIYUN LIN[1], ZHUOLING LI[1], XINYING QIAN[1], HUAQIN ZHANG[1] and YINGLAN ZHAO[1]

[1]Pharmacodynamics Pharmacokinetics Early Safety Evaluation Model Animals, Cancer Center, West China Hospital, Sichuan University and Collaborative Innovation Center; [2]Analytical and Testing Center, Sichuan University, Chengdu, Sichuan 610041, P.R. China

Received December 19, 2016; Accepted June 26, 2017

DOI: 10.3892/or.2017.5954

Abstract. Lung metastasis is an important cause for the low 5-year survival rate of colorectal cancer patients. Understanding the metabolic profile of lung metastasis of colorectal cancer is important for developing molecular diagnostic and therapeutic approaches. We carried out the metabonomic profiling of lung tissue samples on a mouse lung metastasis model of colorectal cancer using ^{1}H-nuclear magnetic resonance (^{1}H-NMR). The lung tissues of mice were collected at different intervals after marine colon cancer cell line CT-26 was intravenously injected into BALB/c mice. The distinguishing metabolites of lung tissue were investigated using ^{1}H-NMR-based metabonomic assay, which is a highly sensitive and non-destructive method for biomarker identification. Principal component analysis (PCA), partial least squares discriminant analysis (PLS-DA) and orthogonal partial least squares discriminant analysis (OPLS-DA) were applied to analyze ^{1}H-NMR profiling data to seek potential biomarkers. All of the 3 analyses achieved excellent separations between the normal and metastasis groups. A total of 42 metabolites were identified, ~12 of which were closely correlated with the process of metastasis from colon to lung. These altered metabolites indicated the disturbance of metabolism in metastatic tumors including glycolysis, TCA cycle, glutaminolysis, choline metabolism and serine biosynthesis. Our findings firstly identified the distinguishing metabolites in mouse colorectal cancer lung metastasis models, and indicated that the metabolite disturbance may be associated with the progression of lung metastasis from colon cancer. The altered metabolites may be potential biomarkers that provide a promising molecular approach for clinical diagnosis and mechanistic study of colorectal cancer with lung metastasis.

Correspondence to: Professor Yinglan Zhao, Pharmacodynamics Pharmacokinetics Early Safety Evaluation Model Animals, Cancer Center, West China Hospital, Sichuan University and Collaborative Innovation Center, Chengdu, Sichuan 610041, P.R. China
E-mail: zhaoyinglan@scu.edu.cn

*Contributed equally

Abbreviations: ^{1}H-NMR, ^{1}H nuclear magnetic resonance; PCA, principal component analysis; PLS-DA, partial least squares discriminant analysis; OPLS-DA, orthogonal partial least squares discriminant analysis; TCA, tricarboxylic acid cycle; CSCs, cancer stem cells; PC, phosphocholine; FC, fold-change

Key words: colorectal cancer, metabolomic profiling, lung metastasis, ^{1}H-NMR, biomarker

Introduction

Colorectal cancer is one of the most malignant cancers and the third cause of cancer-related mortality worldwide (1). Patients with colon cancer (10-30%) have the tendency to develop lung metastasis (2). Due to the lung metastasis of colon cancer, the 5-year survival rate of colon cancer patients is very low. The prevention and early identification of lung metastasis in colorectal cancer patients may significantly enhance survival rates. Therefore, biomarkers that facilitate the early diagnosis of lung metastasis are highly valuable, and investigating the potential biomarkers, which are closely associated with the progression of lung metastasis from colorectal cancer, is an urgent aim of research.

Although distant metastasis is the major cause of colorectal cancer-related mortality and a large number of colorectal cancer patients develop lung metastasis after treatment, little research has focused on the biomarker detection of lung metastasis from colon cancer. Gorlick *et al* showed that colorectal cancer metastasis to the lung has a higher thymidylate synthase (TS) level than liver metastasis (3), and increased levels of E2F lead to increased TS expression in the lung metastasis of colorectal cancer (4). In addition, overexpression of HOXB9 was found to promote metastasis in colon cancer and stable knockdown of HOXB9 reduced the liver and lung metastasis of colon cancer *in vivo* (5). Increasing evidence suggests that cancer stem cells (CSCs) play a crucial role in cancer metastasis (6). Cancer metastasis requires the seeding and successful colonization of CSCs at distant organs (7), and cell surface marker CDCP1 promotes the adhesion of CRC cells to the

lung endothelium (8). Although there are various studies that have investigated the biomarkers for colorectal cancer lung metastasis, the underlying mechanism remains unclear.

Metabonomics is a relatively new technique that is rapidly gaining importance. It is an emerging field of research downstream of transcriptomics, genomics and proteomics. The critical purpose of metabonomics is to determine thousands of small molecules in cells, tissues, organs or biological fluids followed by the application of a series of analytical methods such as nuclear magnetic resonance, color spectrum and mass spectrogram (9). Among these analytical technologies, NMR is an ideal instrumental platform for metabolic analysis since it offers essentially universal detection, excellent quantitative precision, and the potential for high throughput screening (>100 samples/day is attainable). In contrast to classical biochemical approaches, which often focus on a single metabolite or single metabolic reaction, metabonomics involves the collection of quantitative data on a broad series of metabolites in an attempt to acquire an overall understanding of metabolism or metabolic dynamics associated with diseases or different stages of diseases. NMR-based metabonomics is widely applied to identify potential biomarkers of cancers, such as gastric (10), breast (11), esophageal (12), colorectal (13,14) and bladder cancer (15). However, little research has focused on the metabonomic profiling of cancer metastasis. To date, only 3 NMR-based metabonomic studies concerning metastasis have been reported including advanced metastatic breast cancer (11), rat hepatocellular carcinoma (16) and renal cell carcinoma metastasis (17), which suggest that alterations in metabolism such as glycolysis, the choline pathway, TCA cycle and glutamine metabolism occur during cancer metastasis. No research has reported the metabolic profiling of colon cancer with the lung metastasis process, to date.

In the present study, we established a murine lung metastasis model of colorectal cancer by an intravenous injection of the murine colorectal cancer cell line CT26 into mice. We applied ^{1}H-NMR to study the metabonomic profiling of mouse lung tissues and identified 42 distinguishing metabolites between the metastasis and normal control groups. Among the 42 distinguishing metabolites, 12 were closely related with the progression of metastasis. Our results indicate that tumor metabolism including glycolysis, glutamine metabolism, and TCA cycle and choline metabolism play a critical role in the mouse colon cancer lung metastasis process. The altered metabolites could be potential biomarkers, which can provide a promising molecular diagnostic approach for the clinical diagnosis and treatment of colon cancer patients with lung metastasis.

Materials and methods

Animals. Syngeneic BALB/c mice (6-8 weeks of age) were obtained from the Beijing Animal Center (Beijing, China) and housed under controlled environmental conditions. The animals (SPF) were maintained at 21˚C in 55% humidity, on a 12-h light/12-h dark cycle. All animals were housed in a standard animal laboratory allowing free activity and were provided with standard food and water *ad libitum*. All animal procedures were performed according to the National Institutes of Health Guide for the Care and Use of Laboratory Animals. All of the animal protocols were reviewed and approved by the Experimental Animal Ethics Committee of Sichuan University (Chengdu, China).

Reagents. Sodium-3-(trimethylsilyl)-2,2,3,3-tetradeuteriopropionate (TSP) was purchased from Sigma-Aldrich (St. Louis, MO, USA). Deuterium oxide (99.8% D) was purchased from Norell®, Inc. (Landisville, NJ, USA). Methanol and chloroform ($CDCl_3$) were purchased from Fisher Scientific (Fairlawn, NJ, USA). Deionized water was obtained from an EASYpure II UV water purification system (Barnstead International, Dubuque, IA, USA).

Cell culture and in vivo lung metastasis model. CT26 (mouse colorectal carcinoma cell line) was purchased from the American Type Culture Collection (ATCC; Manassas, VA, USA), and was cultured in RPMI-1640 medium supplemented with 10% heat-inactivated fetal bovine serum (FBS) (Gibco, Grand Island, NY, USA), 100 U/ml penicillin and 100 U/ml streptomycin at 37˚C in a humidified atmosphere with 5% CO_2. Cells were passaged at least 2 or 3 times before use.

BALB/c mice (6-8 weeks of age) were used in the present study. Mice in the lung metastasis groups were injected with CT26 cells ($2x10^6$ cells/mouse) via tail vein, and they were sacrificed, 7, 14 and 21 days after cell injection, respectively. Mice in the control group were injected with saline via tail vein. Lung tissues were collected and stored at -80˚C in formalin for subsequent experiments.

Sample preparation for NMR spectroscopy. Lung tissues of mice were carefully microdissected to ensure that the analyzed tissue contained cancer cells. An amount of 200-500 mg of frozen tissue samples was weighed and suspended in methanol (4 ml/g of tissue) and double distilled water (0.85 ml/g of tissue). The suspension was homogenized with 20 strokes at 800 rpm, and chloroform (2 ml/g of tissue) was added, followed by addition of 50% chloroform (2 ml/g of tissue) and homogenization was repeated. The sample was left on ice for 30 min, and centrifuged at 1,000 x g for 30 min at 4˚C. Then, the sample was separated to 3 phases: a water phase at the top, a denatured protein phase in the middle and a lipid phase at the bottom. The water phase of each specimen was collected and evaporated to dryness under a stream of nitrogen. The residue was reconstituted with 580 μl D_2O containing 30 μM phosphate-buffered solution (PBS; pH=7.4) and 0.01 mg/ml sodium-3-(trimethylsilyl)-2,2,3,3-tetradeuteriopropionate (TSP) as an internal standard (δ0.0). After centrifugation at 12,000 x g for 5 min, the supernatant was transferred into a 5-mm NMR tube for NMR spectroscopy (18).

^{1}H-NMR spectroscopic analysis. All tissue samples were analyzed using ^{1}H-NMR spectroscopy at 600.13 MHz using a Bruker Avance II 600 spectrometer operating (Bruker BioSpin, Rheinstetten, Germany) at 300 K. A one-dimensional spectrum was acquired using a standard (1D) Carr-Purcell-Meiboom-Gill (CPMG) pulse sequence to suppress the water signal with a relaxation delay of 5 sec. Sixty-four-free induction decays (FIDs) were collected into 64 K data points with a spectral width of 12,335.5-Hz spectral, an acquisition time of

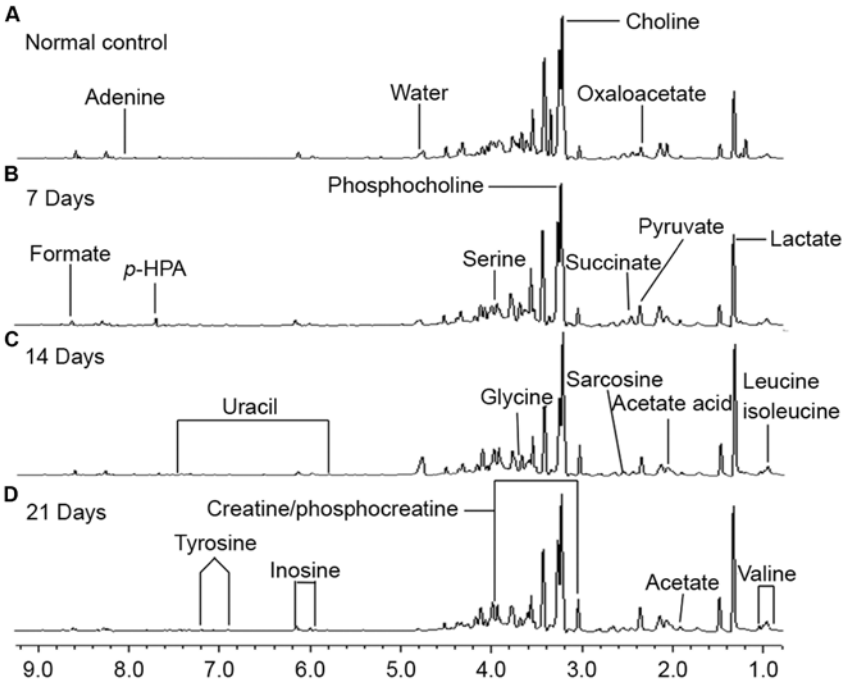

Figure 1. 600 MHz representative ^{1}H-NMR spectra (δ9.5-δ0.5) of lung tissue samples. (A) Normal control. (B) Seven days after injection. (C) Fourteen days after injection. (D) Twenty-one days after injection.

2.66 sec, and a total pulse recycle delay of 7.66 sec. The FIDs were weighted by a Gaussian function with line-broadening factor 20.3 Hz, Gaussian maximum position 0.1, prior to Fourier transformation (19).

Data processing. All NMR data acquired above were subjected to pattern recognition (PR) analysis. Before doing this, the raw data were manually Fourier transformed using MestReNova-6.1.1-6384 software. After phase adjustment and baseline correction, the NMR data were referenced to the TSP resonance at δ0.0. The whole spectrum was divided into 4,500 segments with equal width (0.002 ppm) ranging from 9.5 to 0.5 ppm. The region 5.1-4.7 ppm was removed to exclude the effect of imperfect water suppression. Finally, the data were normalized to eliminate the dilution or bulk mass difference among samples and to give the same total integration value for each spectrum before analysis.

PR analysis. Multivariate analysis was carried out using SIMCA-P + 11 (Umetrics AB, Umeå, Sweden). Principal component analysis (PCA), the unsupervised PR method, was initially applied to analyze the NMR data to separate the lung metastasis nodule samples from normal lung tissues. Partial least squares discriminant analysis (PLS-DA) and orthogonal partial least squares discriminant analysis (OPLS-DA), supervised PR method, were used to improve the separation of the different groups. The PLS-DA model was cross-validated by permutation analysis (200 times) (20,21).

The default 7-round cross validation was applied with 1/7 of the samples being excluded from the mathematical model in each round, in order to guard against over fitting. R^2 and Q^2 were acquired from the PLS-DA model. The variable importance in the projection (VIP) values of all peaks obtained from the OPLS-DA model was analyzed, and only VIP >1 were considered relevant for group discrimination (22). Otherwise, unpaired Student's t-test ($p<0.05$) was also used to assess the significance of each metabolite. With both VIP and p-value meeting the requirements, the metabolites were identified as distinguishing metabolites. The corresponding chemical shift of metabolites was acquired through previous literature and the Human Metabolome Database (http://www.hmdb.ca/).

Results

Construction of the lung metastasis model and metabolic profiling of the samples. CT26 cells were injected into the tail vein of BALB/c mice to construct the metastasis model. Then, the lung tissues were collected at 7, 14 and 21 days after cell injection; on the first day of the experiment the specimens of the normal group were also collected without cell injection.

The collected samples underwent extraction, and the aqueous fractions were investigated using NMR. The typical ^{1}H-NMR spectra of the aqueous phase extracts of lung tissues of the different groups are shown in Fig. 1. The standard one-dimension spectrum provided an overview of all and the major metabolites in the integrated regions were identified according to the literature data and the Human Metabolome Database (http://www.hmdb.ca/). Finally, a series of metabolites which were altered at endogenous metabolite levels were observed in the metastasis groups at 7, 14 and 21 days when compared with the normal group. The different metabolites included amino acids, carbohydrates and lipids which are known to be related with metabolic processes, particularly in energy metabolism (23).

PR analysis of the normal and different metastasis groups. Identification of the different metabolites between the normal and metastasis groups was critical for identifying

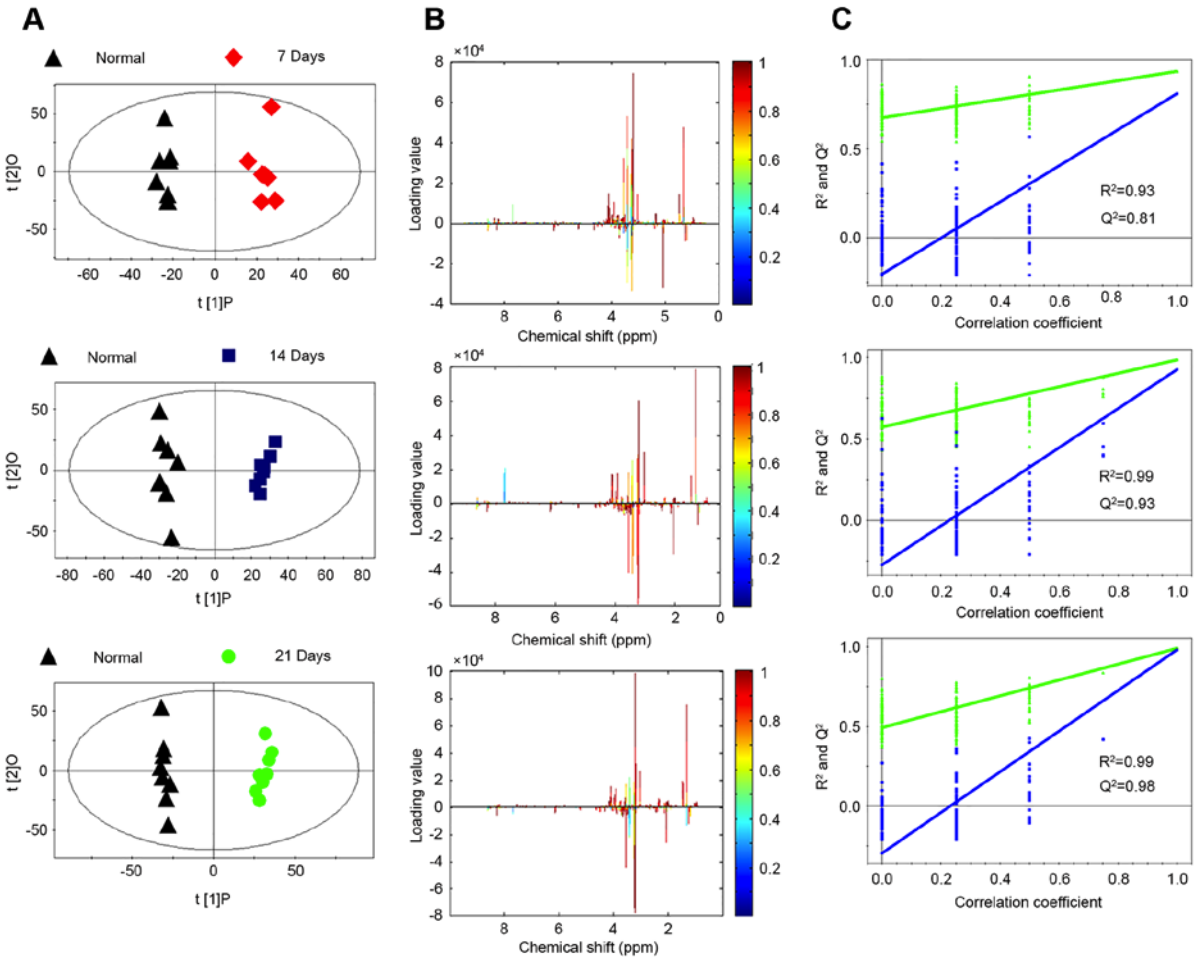

Figure 2. PR analyses of ^{1}H-NMR spectra between the different metastasis groups and normal control. (A) Score plots of OPLS-DA model processing based on the normal group and each metastasis group; red diamonds represent 7 days after injection group; blue boxes represent 14 days after injection group; green dots represent 21 days after injection group. (B) Color map shows the significance of metabolite variations between the groups. Peaks in the positive direction indicate the increased metabolites in the metastasis groups. Peaks in the negative direction represent the decreased metabolites. (C) Statistical validation of the corresponding PLS-DA model by permutation analysis (200 times). R^2 is the explained variance, and Q^2 is the predictive ability of the model.

biomarkers that may be useful for diagnosis and therapy of colon cancer patients who have lung metastasis. OPLS-DA analysis was used to investigate differences in metabolites between the normal and metastasis groups. The scores of PC1 and PC2 showed that each metastasis group including 7, 14 and 21 days after injection were clearly separated from the normal group (Fig. 2A). To identify the distinguishing metabolites, their scores and loading plots were obtained from the OPLS-DA analysis (Fig. 2B). The loadings were colored according to the UV model variable weights and the signals in the positive direction indicate upregulated metabolites, the negative signals represent downregulated metabolites in the metastasis groups compared to the normal group. The PLS-DA model was applied and the statistical validation of the corresponding PLS-DA model was carried out by permutation analysis. The parameters of the different metastasis groups were as follows: 7 days, R^2=0.92 Q^2=0.84; 14 days, R^2=0.98 Q^2=0.94; 21 days, R^2=0.99 Q^2=0.98 (Fig. 2C). The results indicated that each model was suitable for data analysis. We summarized the distinguishing metabolites between the normal and metastasis groups (Tables I and II).

As shown in Table II, acetic acid, choline, creatine, glutamate, glyceryl, glycolate, inosine, isoleucine, lactate, leucine, *N*-acetyl glycoprotein, oxaloacetate, phosphocholine (PC), phosphocreatine, *p*-HPA, pyruvate, serine, threonine, tyrosine, uracil, valine and β-hydroxybutyrate were upregulated in the metastasis groups compared with the normal group. While dimethylamine, glutamine, glycine, *O*-acetyl glycoprotein, sarcosine and succinate were downregulated in the metastasis groups. Many of them increased along with the stage of metastasis. Choline and PC were significantly high in the 7 day group. In addition, *O*-acetyl glycoprotein decreased obviously with a fold-change (FC) >2.5 in each metastasis group compared to the normal group.

Trending biomarkers. Biomarker identification is important for the detection, diagnosis and treatment of cancer, and is also meaningful to investigate the metastatic process of colon cancer to the lung. We used box-and-whisker plots, which included the concentration ranges, median quartiles and extremes to show the representative metabolites of the previously identified 42 metabolites between the normal and metastasis groups (Fig. 3). A heat map showing the relative abundances of the metabolites is shown in Fig. 4.

Most cancer cells prefer the glycolysis pathway to generate energy even with an adequate oxygen supply; thus, the

Table I. Differential metabolites derived from the OPLS-DA model of ^{1}H-NMR analysis between the normal control and metastasis groups.

No.	Metabolite	Multiplicity[a]	Chemical shift (ppm)	Normal vs. metastasis groups		
				VIP[b]	P-value[c]	FC[d]
1	VLDL: C<u>H</u>3-$(CH_2)_{n-}$	br	0.89	1.68	0.0074	-1.08
2	Acetate	s	1.93	1.67	0.0001	1.22
3	Acetic acid	s	2.08	2.29	0.0000	1.67
4	Acetone	s	2.23	1.27	\	-1.04
5	Adenine	m	8.12	1.01	\	-1.65
6	Alanine	d	1.48	1.96	0.0000	1.61
		d	3.76	1.78	0.0018	1.06
7	Arginine	t	3.25	1.24	\	-1.11
8	CH_2OCOR	m	4.17	2.33	0.0000	1.73
9	Choline	s	3.2	1.52	0.0001	1.72
10	Creatine	s	3.04	2.02	0.0000	1.87
		s	3.94	1.90	0.0000	1.49
11	Dimethylamine	s	2.73	2.04	0.0012	-1.29
12	D-ribose	s	2.23	1.27	\	-1.04
13	Ethanol	t	1.19	1.53	0.0090	-2.13
		q	3.67	2.32	0.0000	-1.32
14	Formate	s	8.45	1.42	\	-1.05
15	Fumarate	s	6.53	1.50	\	1.19
16	Glutamate	m	2.35	2.01	0.0000	1.48
17	Glutamine	m	2.14	1.81	0.0001	-1.05
		m	2.45	2.05	0.0003	-1.55
18	Glutathione	m	2.96	0.90	\	1.16
19	Glyceryl	m	4.17	2.33	0.0000	1.73
20	Glycine	s	3.57	1.63	0.0492	-1.04
21	Glycolate	s	3.93	1.90	0.0000	1.49
22	Inosine	d	6.11	1.99	0.0001	2.20
		s	8.36	\	\	1.96
23	Isoleucine	t	0.95	2.10	0.0000	1.63
24	Lactate	d	1.33	2.12	0.0001	1.54
		q	4.11	2.03	0.0000	2.06
25	Leucine	t	0.96	2.14	0.0000	1.78
		d	1.01	2.09	0.0003	1.81
26	Lysine	m	3.77	1.78	0.0018	1.05
27	*N*-acetyl glycoprotein	s	2.04	2.20	0.0000	1.55
28	*O*-acetyl glycoprotein	s	2.07	1.86	0.0001	-2.80
29	Oxaloacetate	s	2.35	2.01	0.0000	1.61
30	Phosphochline	s	3.21	1.52	0.0001	1.72
31	Phosphocreatine	s	3.04	2.02	0.0000	1.87
		s	3.93	1.90	0.0000	1.49
32	*p*-HPA	s	3.9	1.90	0.0000	1.49
		m	7.28	1.72	\	1.03
		d	7.51	2.36	0.0000	5.00
		d	7.71	1.95	0.0000	2.42
33	Pyruvate	s	2.37	1.80	0.0000	1.38
34	Sarcosine	s	2.75	1.83	0.0082	-1.36
35	Serine	m	3.98	2.35	0.0000	1.45
36	Succinate	s	2.41	1.64	0.0102	-1.63
37	Taurine	t	3.27	1.24	\	-1.11
		t	3.43	1.24	0.0100	-1.11
38	Threonine	m	4.24	2.00	0.0008	1.21

Table I. Continued.

No.	Metabolite	Multiplicity[a]	Chemical shift (ppm)	Normal vs. metastasis groups		
				VIP[b]	P-value[c]	FC[d]
39	Tyrosine	d	6.9	2.15	0.0001	1.53
		d	7.2	2.20	0.0000	1.48
40	Uracil	d	5.8	2.38	0.0000	12.15
		d	7.54	2.36	0.0000	5.00
41	Valine	d	0.99	2.02	0.0000	1.43
		d	1.05	2.21	0.0002	1.49
42	β-hydroxybutyrate	m	4.16	2.33	0.0000	1.73

[a]Multiplicity: s, singlet; d, doublet; t, triplet; q, quartet; dd doublet of doublets, m multiplet. [b]Variable importance in the projection was obtained from OPLS-DA model with a threshold of 1.0. [c]p-value obtained from Student's t-test. [d]Fold-change (FC) between normal and metastasis groups. Fold-change with a positive value indicates a relatively higher concentration present in metastasis groups while a negative value means a relatively lower concentration as compared to the normal group. OPLS-DA, orthogonal partial least squares discriminant analysis; ^{1}H-NMR, ^{1}H nuclear magnetic resonance; VIP, variable importance in the projection; FC, fold-change.

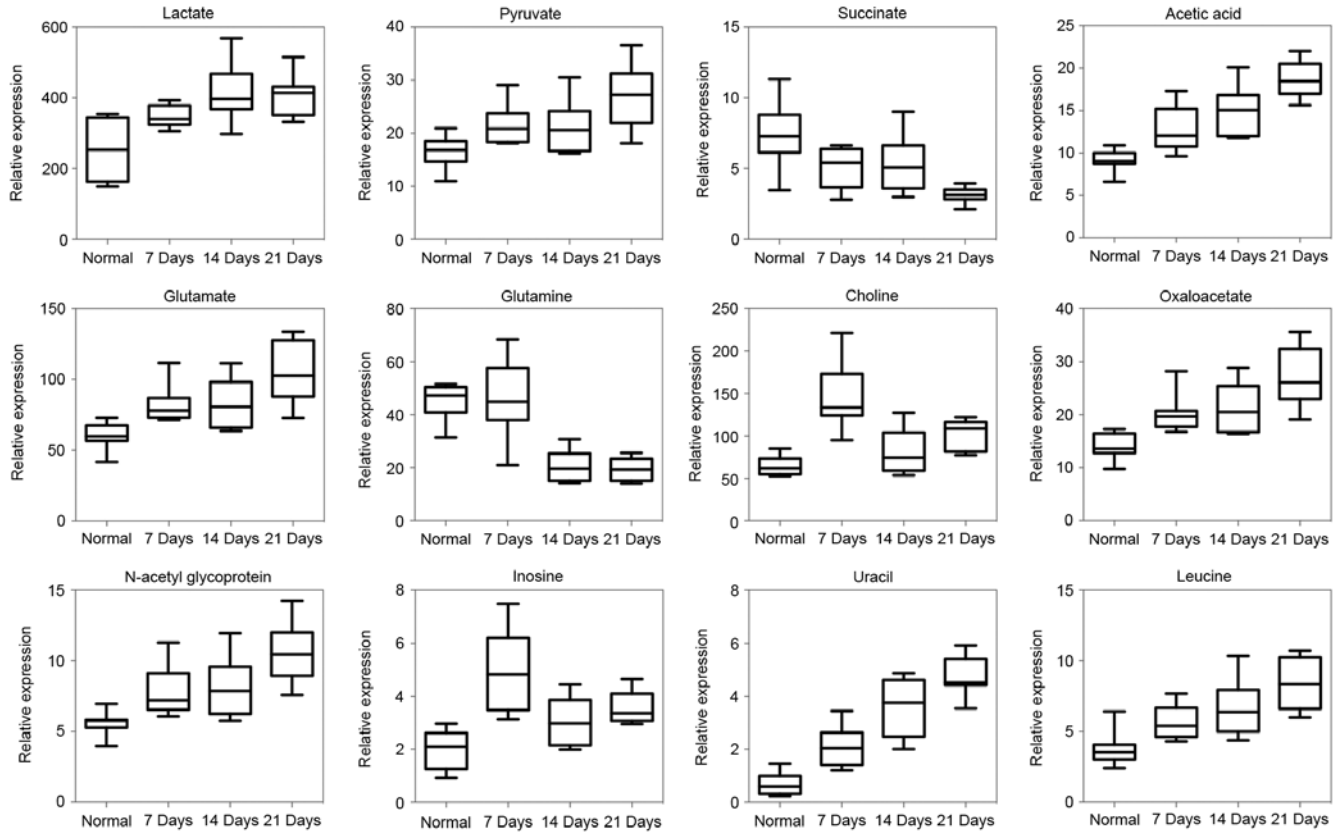

Figure 3. Box-and-whisker plots illustrate progressive changes of the metabolites between the normal group and metastasis groups. Horizontal line in the middle portion of the box, median; bottom and top boundaries of boxes, lower and upper quartile; whiskers, 5th and 95th percentiles; open circles, outliers.

increased level of lactate in the tumor tissue was not surprising. Furthermore, research has shown that a high lactate concentration is associated with metastasis of tumors consistent with the present study (24,25). Pyruvate, an important product of glycolysis, is increased along with the progression of colon cancer metastasis to the lung, which is a good indicator of active glycogenolysis and glycolysis. Oxaloacetate was also found to be upregulated, which may be due to the activity of pyruvate carboxylase catalyzing the pyruvate which is converted to oxaloacetate. Meanwhile, succinate was obviously downregulated, which suggests that dysregulation of the TCA cycle may be correlated with the lung metastasis of colorectal cancer.

In the present study, glutamate was significantly increased in the metastasis group compared with that in the normal group. It has been reported that glutamate is upregulated in

Table II. Summary of the different metabolites between each metastasis and normal group.

Metabolite	Multiplicity[a]	Chemical shift (ppm)	Normal vs. 7 days			Normal vs. 14 days			Normal vs. 21 days		
			VIP[b]	P-value[c]	FC[d]	VIP[b]	P-value[c]	FC[d]	VIP[b]	P-value[c]	FC[d]
VLDL: $C\underline{H}_3$-$(CH_2)_{n-}$	br	0.89	1.41	0.034	1.07	1.75	0.001	-1.21	1.50	0.002	-1.14
Acetate	s	1.93	1.42	0.028	1.35	1.72	0.002	1.04	1.77	<0.001	1.29
Acetic acid	s	2.08	1.86	0.002	1.39	2.11	<0.001	1.61	2.00	<0.001	2.05
Acetone	s	2.23	1.32	0.040	1.09	1.15	0.074	-1.22	1.54	0.001	-1.02
Adenine	m	8.12	1.21	\	-1.53	1.70	0.007	-2.22	1.20	0.022	-1.38
Alanine	d	1.48	2.21	<0.001	1.42	1.78	0.001	1.62	1.83	<0.001	1.82
	d	3.76	1.86	0.003	1.08	1.96	<0.001	-1.01	1.76	<0.001	1.12
Arginine	t	3.25	1.27	\	1.07	1.74	0.001	-1.29	1.14	0.028	-1.19
CH_2OCOR	m	4.17	2.02	<0.001	1.42	2.06	<0.001	1.63	2.01	<0.001	2.21
Choline	s	3.2	2.37	<0.001	2.26	1.71	0.002	1.30	1.86	<0.001	1.58
Creatine	s	3.04	1.80	0.004	1.42	2.17	<0.001	2.07	1.86	<0.001	2.14
	s	3.94	1.86	0.002	1.35	2.04	<0.001	1.58	1.88	<0.001	1.55
Dimethylamine	s	2.73	1.82	0.009	-1.04	2.08	<0.001	-1.71	1.78	<0.001	-1.29
D-ribose	s	2.23	1.32	0.040	1.09	1.15	\	-1.22	1.54	0.001	-1.02
Ethanol	t	1.19	1.54	0.036	-2.30	1.67	0.007	-1.93	1.52	0.004	-2.19
	q	3.67	1.69	0.018	-1.04	2.01	<0.001	-1.37	1.99	<0.001	-1.78
Formate	s	8.45	1.47	0.035	-1.08	1.27	\	-1.05	1.29	0.012	-1.02
Fumarate	s	6.53	1.96	0.001	1.33	1.51	0.007	1.06	1.73	<0.001	1.18
Glutamate	m	2.35	2.11	<0.001	1.44	1.69	0.002	1.35	1.88	<0.001	1.73
Glutamine	m	2.14	1.56	0.013	1.07	2.14	<0.001	-1.19	1.80	<0.001	-1.04
	m	2.45	\	\	1.03	2.19	<0.001	-2.18	1.98	<0.001	-2.33
Glutathione	m	2.96	1.87	0.002	1.29	1.25	0.038	1.08	\	\	1.10
Glyceryl	m	4.17	2.02	<0.001	1.42	2.06	<0.001	1.63	2.01	<0.001	2.21
Glycine	s	3.57	1.65	0.008	1.28	1.64	0.003	-1.24	1.79	<0.001	-1.28
Glycolate	s	3.93	1.86	0.002	1.35	2.04	<0.001	1.58	1.88	<0.001	1.55
Inosine	d	6.11	1.99	0.001	2.24	1.90	<0.001	1.96	1.98	<0.001	2.41
	s	8.36	2.27	<0.001	2.50	1.45	0.011	1.56	1.38	0.006	1.82
Isoleucine	t	0.95	2.09	0.001	1.48	1.88	<0.001	1.56	1.89	<0.001	1.88
Lactate	d	1.33	1.63	0.011	1.37	2.09	<0.001	1.64	1.88	<0.001	1.61
	q	4.11	2.08	<0.001	1.86	2.12	<0.001	2.24	1.93	<0.001	2.10
Leucine	t	0.96	2.11	<0.001	1.55	1.88	<0.001	1.71	1.89	<0.001	2.12
	d	1.01	1.72	0.009	1.50	1.80	0.001	1.75	1.90	<0.001	2.22
Lysine	m	3.77	2.00	<0.001	1.16	1.96	<0.001	-1.01	1.76	<0.001	1.05
N-acetyl glycoprotein	s	2.04	1.70	0.005	1.39	1.91	<0.001	1.43	1.95	<0.001	1.88
O-acetyl glycoprotein	s	2.07	2.41	<0.001	-2.90	2.22	<0.001	-3.10	1.88	<0.001	-2.44
Oxaloacetate	s	2.35	1.96	0.001	1.37	1.67	0.002	1.50	1.88	<0.001	1.94
Phosphochline	s	3.21	2.37	<0.001	2.26	1.71	0.002	1.30	1.86	<0.001	1.58
Phosphocreatine	s	3.04	1.80	0.004	1.42	2.17	<0.001	2.07	1.86	<0.001	2.14
	s	3.93	1.86	0.002	1.35	2.04	<0.001	1.58	1.88	<0.001	1.55
p-HPA	s	3.9	1.86	0.002	1.35	2.04	<0.001	1.58	1.88	<0.001	1.55
	m	7.28	1.95	0.001	1.17	1.84	0.001	-1.09	1.69	<0.001	1.01
	d	7.51	2.26	<0.001	3.01	2.10	<0.001	5.22	2.02	<0.001	6.98
	d	7.71	2.22	<0.001	2.31	1.90	<0.001	3.06	1.73	<0.001	1.81
Pyruvate	s	2.37	2.09	<0.001	1.30	1.71	0.001	1.26	1.81	<0.001	1.62
Sarcosine	s	2.75	1.03	\	1.02	1.92	0.001	-2.10	1.57	0.003	-1.44
Serine	m	3.98	2.31	<0.001	1.30	2.07	<0.001	1.40	2.04	<0.001	1.67
Succinate	s	2.41	1.70	0.015	-1.45	1.41	0.023	-1.41	1.70	0.001	-2.38
Taurine	t	3.27	1.27	\	1.07	1.74	0.001	-1.29	1.14	0.028	-1.19
	t	3.43	1.77	0.012	1.06	1.78	0.005	-1.28	1.19	0.025	-1.17
Threonine	m	4.24	1.77	<0.001	1.14	2.06	<0.001	1.12	1.91	<0.001	1.39

Table II. Continued.

Metabolite	Multiplicity[a]	Chemical shift (ppm)	Normal vs. 7 day			Normal vs. 14 day			Normal vs. 21 day		
			VIP[b]	P-value[c]	FC[d]	VIP[b]	P-value[c]	FC[d]	VIP[b]	P-value[c]	FC[d]
Tyrosine	d	6.9	1.85	0.007	1.48	1.91	<0.001	1.43	1.93	<0.001	1.69
	d	7.2	2.03	<0.001	1.47	2.03	<0.001	1.37	1.96	<0.001	1.61
Uracil	d	5.8	2.24	<0.001	6.29	2.16	<0.001	12.44	2.06	<0.001	18.43
	d	7.54	2.26	<0.001	3.01	2.10	<0.001	5.22	2.02	<0.001	6.98
Valine	d	0.99	1.49	0.018	1.24	1.68	0.003	1.43	1.87	<0.001	1.65
	d	1.05	1.59	0.011	1.21	1.78	0.001	1.42	1.93	<0.001	1.89
β-hydroxybutyrate	m	4.16	2.02	<0.001	1.42	2.06	<0.001	1.63	2.01	<0.001	2.21

[a]Multiplicity: s, singlet; d, doublet; t, triplet; q, quartet; dd, doublet of doublets; m, multiplet. [b]Variable importance in the projection was obtained from OPLS-DA model with a threshold of 1.0. [c]P-value obtained from Student's t-test. [d]Fold-change (FC) between normal and metastasis groups. Fold-change with a positive value indicates a relatively higher concentration present in metastasis groups while a negative value means a relatively lower concentration as compared to the normal group. \, represents this parameter is not statistically significant. VIP, variable importance in the projection.

many types of cancers and high levels of glutamate may be associated with the activation of glutaminolysis, due to an increased activity of the mitochondrial enzyme glutaminase in metastatic tumors. In addition, research has shown that glutamate levels are increased in pancreatic cancer, which can promote invasion and migration ability via AMPA receptor activation and Kras-MAPK signaling (26). Thus, elevated glutamate levels may contribute to the metastasis of colon cancer and glutamate can be a biomarker for the detection of lung metastasis derived from colon. Due to the activation of glutaminolysis, glutamine is consumed and utilized by colon tumors at much higher rates than other amino acids; thus, glutamine was found to be obviously downregulated in the metastasis group in our research.

As previously mentioned, there are only 3 literature studies that have reported NMR-based metabonomics of metastatic tumors and our results are partly consistent with previous studies. Choline, a basic constituent of lecithin was upregulated in our research owing to an increased rate of metabolism of phospholipids to lipids, or a greater demand for phospholipids to encourage rapid proliferation and aggression of colon cancer cells (27). Wang *et al* analyzed the metabonomics of hepatocellular carcinoma with lung metastasis (HLM) rat models and found that choline was increased in HLM rat models compared with the control group (16).

The concentration of *N*-acetyl glycoproteins in the metastasis groups was higher than that noted in the non-metastasis group and was elevated significantly along with progression. This result was consistent with a previous study concerning advanced metastatic human breast cancer (11). The obvious upregulation of uracil in tissues demonstrated the activation of transcriptions in the process of metastasis to meet the needs of rapid cell proliferation. Then, the high concentration of inosine indicated that the purine metabolism was active in metastatic progression. Leucine, isoleucine and serine were increased in the metastasis group compared with the normal group that satisfy the requirements for structural proteins of cancer cells in metastasis.

Discussion

In the present study, we investigated the metabolic profiling of mouse colorectal cancer with lung metastasis based on ^{1}H-NMR. Forty-two different metabolites were identified and some of them were significantly correlated with the progression of colorectal cancer metastasis to the lung. We summarized the metabolic pathways based on human metabolome database and the Kyoto Encyclopedia of Genes and Genomes (KEGG) and the main disordered pathways included glycolysis, TCA cycle, glutaminolysis, choline metabolism and serine biosynthesis (Fig. 5). To the best of our knowledge, little research has focused on the metabolic profiling of colorectal cancer with lung metastasis. The present study is the first to identify the different metabolites in the lung tissues during the process of metastasis.

We detected metabolites of whole lung between the metastasis groups and normal group due to the 'seed and soil' hypothesis which was proposed by Paget early in 1889 (28). It is well known that sites of metastasis are determined not only by the characteristics of the primary tumor cells, but also by the microenvironment of host tissues (29). Therapy for metastasis should be targeted not only against the cancer cells themselves, but also against the homeostatic factors that promote tumor-cell invasion and metastasis in the tumor microenvironment of specific organs (30). Colorectal cancer patients often develop liver and lung metastasis probably due to the fact that these organs provide suitable soil for colon cancer cell colonization. The change in microenvironment may lead to the disorder of metabolism and we found that the metabolites of whole lung tissue could better reflect the change in the microenvironment during the process of metastasis.

Otto Warburg first observed the alteration of cancer cell metabolism early in 1921. He found that most cancer cells prefer to use glucose at a high level and convert it to lactate instead of relying on mitochondrial oxidative phosphorylation to generate energy even in the presence of abundant oxygen. This is termed the 'Warburg effect' (31). Recent studies

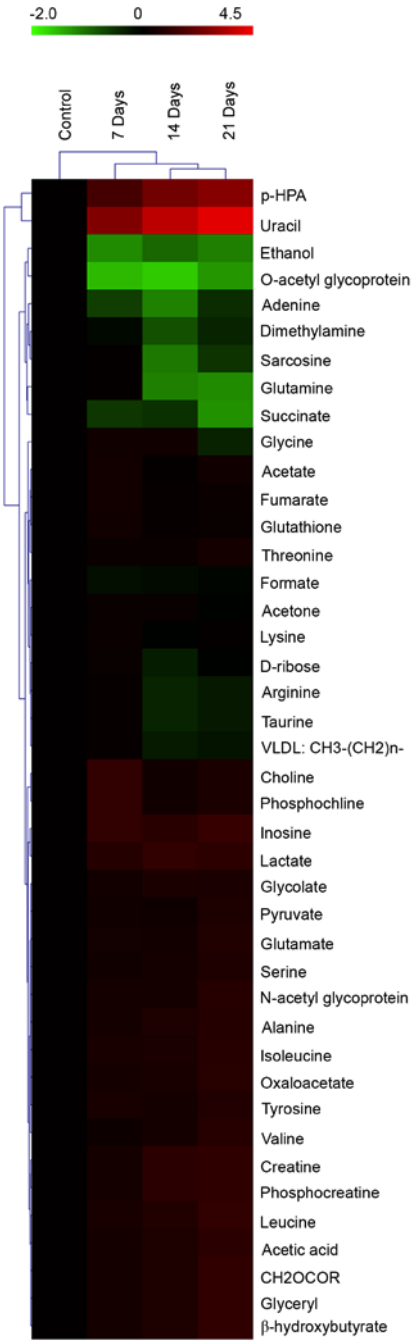

Figure 4. Heat maps of the abundances of metabolites. Heat map showing relative abundances of metabolites between the CT26 injection group and normal controls.

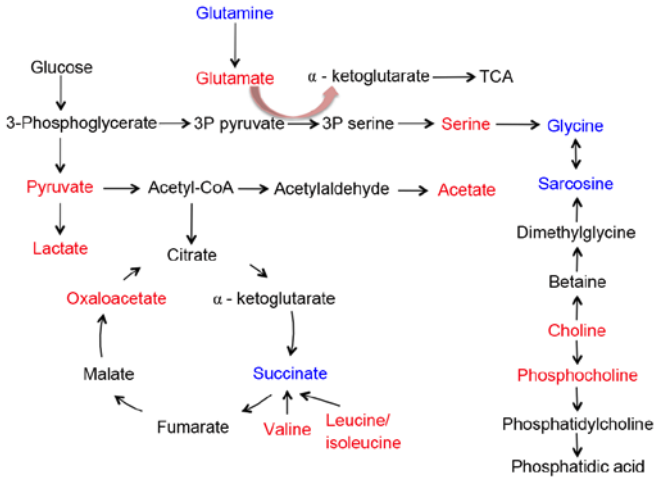

Figure 5. Metabolic pathways of significantly altered metabolites between the CT26 injection group and normal controls. Red represents metabolites that were upregulated in the metastasis groups compared to the normal group. Blue represents metabolites that were downregulated in the metastasis groups compared to the normal group. Boldface indicates not measured or not significant between the two groups.

show that aerobic glycolysis is not only crucial for tumor cell growth, but also essential for tumor cell migration and invasion, which is consistent with the results that the lactate level was significantly high in the metastasis groups. Research has reported that lactate induces secretion of hyaluronan by tumor-associated fibroblasts which create a milieu favorable for migration that benefits tumor metastasis. The high level concentration of lactate leads to normal cell death via caspase-mediated activation of the p53-dependent apoptotic pathway (32), but cancer cells can export lactate by monocarboxylate transporters (MCTs) resulting in the acidification of the microenvironment (33). The low pH of the extracellular environment provides a favorable condition for the activation of proteases, such as matrix metalloproteinases (MMPs) (34), which in turn can help cancer cells degrade the extracellular matrix (ECM) and facilitate metastasis (35). Thus, aerobic glycolysis may increase cancer cell migration and invasiveness due to the disturbance of the microenvironment which is beneficial for their proliferation and metastasis but toxic to normal cells (36). Therefore, the increased lactate in lung tissues could benefit the metastatic ability of colorectal cancer cells.

Pyruvate, the end product of glycolysis, was upregulated in our research and a previous study showed that pyruvate promotes cancer cell metastasis. Anoikis resistance, or the ability of cells to live detached from the EMC, is a property of epithelial cancers. Caneba *et al* found higher pyruvate uptake and oxygen consumption in more invasive ovarian cancer cells than their less invasive counterparts under detached conditions, and pyruvate has an effect on highly invasive ovarian cancer cell migration ability (37).

However, increased aerobic glycolysis, enhanced glutamine metabolism is now considered a key feature of cancer cells and contributes to cancer cell migration. Our research showed moderate downregulation of glutamine and upregulation of glutamate in lung tissues in the metastasis groups compared with the normal group. In cancer cells, glutamine is catabolized to glutamate by glutaminase. Glutamate is then catabolized by glutamate dehydrogenase to α-ketoglutarate to feed the TCA cycle (38). Recent studies suggest that glutamine metabolism contributes to cancer cell migration. Glutamine can support lipogenesis by providing both acetyl-CoA and NADPH, which, in turn, regulates the activation of AKT (39), and the AKT pathway is involved in the migratory and invasive abilities of many cancer cell lines (40,41). In malignant glioma, a high extracellular concentration of glutamate is released, and released glutamate acts as an essential autocrine/paracrine signal that promotes cell invasion (42). Glutamate was also found to promote invasion and migration of pancreatic cancer cells via AMPA receptor activation and K-ras-MAPK

signaling (26). Thus, downregulation of glutamine and upregulation of glutamate in the present study was consistent with above study, and may play an important role in lung metastasis in colorectal cancer.

Abnormal choline metabolism is emerging as a metabolic hallmark that is associated with oncogenesis and tumor progression (43). In the present study, two-choline metabolism pathway-related metabolites (choline/phosphocholine) were upregulated. Previous studies have reported the correlation of choline metabolism, cancer metastasis including breast cancer (44) and hepatocellular carcinoma (16), and malignant transformation (43). Choline is an essential nutrient transported by choline transporters from plasma to cells that can be a rate-limiting step in phosphocholine formation. Phosphocholine is synthesized to phosphatidylcholine, which together with other phospholipids form the characteristic bilayer structure of cellular membranes and regulates membrane integrity (45). When highly malignant breast cancer cells were transfected with metastasis suppressor gene *nm23* (46,47), it was found that the ratio of phosphocholine/glycerocholine was lower than that of the empty vector-transfected cells, also an increase of phosphocholine level was detected in NIH 3T3 cells transfected with mutant ras oncogene (48). Thus, upregulation of choline and phosphocholine in our research may be due to the activating genes that control cell metastasis in the process of metastasis.

The results from our studies showed that serine biosynthesis was also involved in the process of colorectal cancer metastasis to the lung, with the serine concentration in the metastasis groups higher than that in the normal group. A study of Pollari *et al* suggested that 3 genes involved in the L-serine biosynthesis pathway, phosphoglycerate dehydrogenase (PHGDH), phosphoserine aminotransferase 1 (PSAT1) and phosphoserine phosphatase (PSPH) were upregulated in highly metastatic breast cancer cells, which is in agreement with our research (49). PHGDH, which catalyses the first step in the serine biosynthesis pathway, is elevated in 70% of estrogen receptor (ER)-negative breast cancers suggesting that serine biosynthesis is active in malignant tumors (50). Ectopic expression of PHGDH in mammary epithelial cells was found to disrupt acinar morphogenesis and induce other phenotypic alterations that may predispose cells to transformation (51). Similarly, glycine and related metabolites, or their associated metabolic pathways, have been identified as central to cancer metastasis (52) and cellular transformation (50,53).

In addition, we observed the upregulation of leucine, isoleucine and valine in the metastasis group relative to the normal group, which is consistent with published literature that reported decreased expression for genes involved in valine, leucine and isoleucine degradation in metastatic colon cancer (54). However, glucose, branched-chain amino acids (BCCAs) including valine, leucine and isoleucine can serve as energy substrates either (38) in brain interstitial space with lower glucose level than that of blood or when glucose is limited some cells can use amino acids to support their survival (55). Thus, the upregulation of BCCAs in our finding may be due to the rapid consumption of glucose, which meets the energy supply during lung metastasis progression. It is also reported that, BCCAs, particularly leucine, enhance tumor invasiveness through activation of the mammalian target of rapamycin complex 1 (mTORC1). Thus, the increase in BCCAs in the lung may provide a suitable microenvironment for metastatic processes.

In conclusion, in the present study, we analyzed the metabolic profiling of colorectal cancer with lung metastasis compared with a normal control based on ^{1}H-NMR spectroscopy combined with multivariate statistical analysis in a mouse model. We identified the distinguishing metabolites and found that metabolic pathways such as glycolysis, TCA cycle, glutaminolysis, choline metabolism and serine biosynthesis, may be involved in the process of metastasis. The present study provides evidence that tumor metabolism regulation plays a critical role in tumor metastasis; the underlying aberrant metabolic pathways could be considered as novel targets for cancer therapy.

Acknowledgements

The present study was supported by the Project of the National Natural Sciences Foundation of China (nos. 81272459 and 81322035).

References

1. Siegel R, Ma J, Zou Z and Jemal A: Cancer statistics, 2014. CA Cancer J Clin 64: 9-29, 2014.
2. Mitry E, Guiu B, Cosconea S, Jooste V, Faivre J and Bouvier AM: Epidemiology, management and prognosis of colorectal cancer with lung metastases: A 30-year population-based study. Gut 59: 1383-1388, 2010.
3. Gorlick R, Metzger R, Danenberg KD, Salonga D, Miles JS, Longo GS, Fu J, Banerjee D, Klimstra D, Jhanwar S, *et al*: Higher levels of thymidylate synthase gene expression are observed in pulmonary as compared with hepatic metastases of colorectal adenocarcinoma. J Clin Oncol 16: 1465-1469, 1998.
4. Banerjee D, Gorlick R, Liefshitz A, Danenberg K, Danenberg PC, Danenberg PV, Klimstra D, Jhanwar S, Cordon-Cardo C, Fong Y, *et al*: Levels of E2F-1 expression are higher in lung metastasis of colon cancer as compared with hepatic metastasis and correlate with levels of thymidylate synthase. Cancer Res 60: 2365-2367, 2000.
5. Huang K, Yuan R, Wang K, Hu J, Huang Z, Yan C, Shen W and Shao J: Overexpression of HOXB9 promotes metastasis and indicates poor prognosis in colon cancer. Chin J Cancer Res 26: 72-80, 2014.
6. Visvader JE and Lindeman GJ: Cancer stem cells in solid tumours: Accumulating evidence and unresolved questions. Nat Rev Cancer 8: 755-768, 2008.
7. Al-Hajj M and Clarke MF: Self-renewal and solid tumor stem cells. Oncogene 23: 7274-7282, 2004.
8. Gao W, Chen L, Ma Z, Du Z, Zhao Z, Hu Z and Li Q: Isolation and phenotypic characterization of colorectal cancer stem cells with organ-specific metastatic potential. Gastroenterology 145: 636-46.e5, 2013.
9. Kaddurah-Daouk R, Kristal BS and Weinshilboum RM: Metabolomics: A global biochemical approach to drug response and disease. Annu Rev Pharmacol Toxicol 48: 653-683, 2008.
10. Jung J, Jung Y, Bang EJ, Cho SI, Jang YJ, Kwak JM, Ryu DH, Park S and Hwang GS: Noninvasive diagnosis and evaluation of curative surgery for gastric cancer using NMR-based metabolomic profiling. Ann Surg Oncol 21 (Suppl 4): S736-S742, 2014.
11. Jobard E, Pontoizeau C, Blaise BJ, Bachelot T, Elena-Herrmann B and Trédan O: A serum nuclear magnetic resonance-based metabolomic signature of advanced metastatic human breast cancer. Cancer Lett 343: 33-41, 2014.
12. Wang L, Chen J, Chen L, Deng P, Bu Q, Xiang P, Li M, Lu W, Xu Y, Lin H, *et al*: ^{1}H-NMR based metabonomic profiling of human esophageal cancer tissue. Mol Cancer 12: 25, 2013.
13. Wang H, Wang L, Zhang H, Deng P, Chen J, Zhou B, Hu J, Zou J, Lu W, Xiang P, *et al*: ^{1}H NMR-based metabolic profiling of human rectal cancer tissue. Mol Cancer 12: 121, 2013.

14. Farshidfar F, Weljie AM, Kopciuk K, Buie WD, Maclean A, Dixon E, Sutherland FR, Molckovsky A, Vogel HJ and Bathe OF: Serum metabolomic profile as a means to distinguish stage of colorectal cancer. Genome Med 4: 42, 2012.
15. Cao M, Zhao L, Chen H, Xue W and Lin D: NMR-based metabolomic analysis of human bladder cancer. Anal Sci 28: 451-456, 2012.
16. Wang J, Zhang S, Li Z, Yang J, Huang C, Liang R, Liu Z and Zhou R: ^{1}H-NMR-based metabolomics of tumor tissue for the metabolic characterization of rat hepatocellular carcinoma formation and metastasis. Tumour Biol 32: 223-231, 2011.
17. Gao H, Dong B, Jia J, Zhu H, Diao C, Yan Z, Huang Y and Li X: Application of ex vivo ^{1}H NMR metabonomics to the characterization and possible detection of renal cell carcinoma metastases. J Cancer Res Clin Oncol 138: 753-761, 2012.
18. Beckonert O, Keun HC, Ebbels TM, Bundy J, Holmes E, Lindon JC and Nicholson JK: Metabolic profiling, metabolomic and metabonomic procedures for NMR spectroscopy of urine, plasma, serum and tissue extracts. Nat Protoc 2: 2692-2703, 2007.
19. Hu Z, Deng Y, Hu C, Deng P, Bu Q, Yan G, Zhou J, Shao X, Zhao J, Li Y, *et al*: ^{1}H NMR-based metabonomic analysis of brain in rats of morphine dependence and withdrawal intervention. Behav Brain Res 231: 11-19, 2012.
20. Trygg J, Holmes E and Lundstedt T: Chemometrics in metabonomics. J Proteome Res 6: 469-479, 2007.
21. Martin FP, Wang Y, Sprenger N, Yap IK, Lundstedt T, Lek P, Rezzi S, Ramadan Z, van Bladeren P, Fay LB, *et al*: Probiotic modulation of symbiotic gut microbial-host metabolic interactions in a humanized microbiome mouse model. Mol Syst Biol 4: 157, 2008.
22. Jansson J, Willing B, Lucio M, Fekete A, Dicksved J, Halfvarson J, Tysk C and Schmitt-Kopplin P: Metabolomics reveals metabolic biomarkers of Crohn's disease. PLoS One 4: e6386, 2009.
23. Lai HS, Lee JC, Lee PH, Wang ST and Chen WJ: Plasma free amino acid profile in cancer patients. Semin Cancer Biol 15: 267-276, 2005.
24. Brizel DM, Schroeder T, Scher RL, Walenta S, Clough RW, Dewhirst MW and Mueller-Klieser W: Elevated tumor lactate concentrations predict for an increased risk of metastases in head-and-neck cancer. Int J Radiat Oncol Biol Phys 51: 349-353, 2001.
25. Walenta S, Schroeder T and Mueller-Klieser W: Lactate in solid malignant tumors: Potential basis of a metabolic classification in clinical oncology. Curr Med Chem 11: 2195-2204, 2004.
26. Herner A, Sauliunaite D, Michalski CW, Erkan M, De Oliveira T, Abiatari I, Kong B, Esposito I, Friess H and Kleeff J: Glutamate increases pancreatic cancer cell invasion and migration via AMPA receptor activation and Kras-MAPK signaling. Int J Cancer 129: 2349-2359, 2011.
27. Morse DL, Carroll D, Day S, Gray H, Sadarangani P, Murthi S, Job C, Baggett B, Raghunand N and Gillies RJ: Characterization of breast cancers and therapy response by MRS and quantitative gene expression profiling in the choline pathway. NMR Biomed 22: 114-127, 2009.
28. Paget S: The distribution of secondary growths in cancer of the breast. 1889. Cancer Metastasis Rev 8: 98-101, 1989.
29. Hart IR and Fidler IJ: Role of organ selectivity in the determination of metastatic patterns of B16 melanoma. Cancer Res 40: 2281-2287, 1980.
30. Fidler IJ: The pathogenesis of cancer metastasis: The 'seed and soil' hypothesis revisited. Nat Rev Cancer 3: 453-458, 2003.
31. Warburg O, Wind F and Negelein E: The metabolism of tumors in the body. J Gen Physiol 8: 519-530, 1927.
32. Williams AC, Collard TJ and Paraskeva C: An acidic environment leads to p53 dependent induction of apoptosis in human adenoma and carcinoma cell lines: Implications for clonal selection during colorectal carcinogenesis. Oncogene 18: 3199-3204, 1999.
33. Porporato PE, Dhup S, Dadhich RK, Copetti T and Sonveaux P: Anticancer targets in the glycolytic metabolism of tumors: A comprehensive review. Front Pharmacol 2: 49, 2011.
34. Lardner A: The effects of extracellular pH on immune function. J Leukoc Biol 69: 522-530, 2001.
35. Gatenby RA, Gawlinski ET, Gmitro AF, Kaylor B and Gillies RJ: Acid-mediated tumor invasion: A multidisciplinary study. Cancer Res 66: 5216-5223, 2006.
36. Han T, Kang D, Ji D, Wang X, Zhan W, Fu M, Xin HB and Wang JB: How does cancer cell metabolism affect tumor migration and invasion? Cell Adhes Migr 7: 395-403, 2013.
37. Caneba CA, Bellance N, Yang L, Pabst L and Nagrath D: Pyruvate uptake is increased in highly invasive ovarian cancer cells under anoikis conditions for anaplerosis, mitochondrial function, and migration. Am J Physiol Endocrinol Metab 303: E1036-E1052, 2012.
38. DeBerardinis RJ, Mancuso A, Daikhin E, Nissim I, Yudkoff M, Wehrli S and Thompson CB: Beyond aerobic glycolysis: Transformed cells can engage in glutamine metabolism that exceeds the requirement for protein and nucleotide synthesis. Proc Natl Acad Sci USA 104: 19345-19350, 2007.
39. Wang HQ, Altomare DA, Skele KL, Poulikakos PI, Kuhajda FP, Di Cristofano A and Testa JR: Positive feedback regulation between AKT activation and fatty acid synthase expression in ovarian carcinoma cells. Oncogene 24: 3574-3582, 2005.
40. Shih MC, Chen JY, Wu YC, Jan YH, Yang BM, Lu PJ, Cheng HC, Huang MS, Yang CJ, Hsiao M, *et al*: TOPK/PBK promotes cell migration via modulation of the PI3K/PTEN/AKT pathway and is associated with poor prognosis in lung cancer. Oncogene 31: 2389-2400, 2012.
41. Walker L, Millena AC, Strong N and Khan SA: Expression of TGFβ3 and its effects on migratory and invasive behavior of prostate cancer cells: Involvement of PI3-kinase/AKT signaling pathway. Clin Exp Metastasis 30: 13-23, 2013.
42. Ishiuchi S, Tsuzuki K, Yoshida Y, Yamada N, Hagimura N, Okado H, Miwa A, Kurihara H, Nakazato Y, Tamura M, *et al*: Blockage of Ca^{2+}-permeable AMPA receptors suppresses migration and induces apoptosis in human glioblastoma cells. Nat Med 8: 971-978, 2002.
43. Glunde K, Bhujwalla ZM and Ronen SM: Choline metabolism in malignant transformation. Nat Rev Cancer 11: 835-848, 2011.
44. Gadiya M, Mori N, Cao MD, Mironchik Y, Kakkad S, Gribbestad IS, Glunde K, Krishnamachary B and Bhujwalla ZM: Phospholipase D1 and choline kinase-α are interactive targets in breast cancer. Cancer Biol Ther 15: 593-601, 2014.
45. Mountford CE and Wright LC: Organization of lipids in the plasma membranes of malignant and stimulated cells: A new model. Trends Biochem Sci 13: 172-177, 1988.
46. Bhujwalla ZM, Aboagye EO, Gillies RJ, Chacko VP, Mendola CE and Backer JM: Nm23-transfected MDA-MB-435 human breast carcinoma cells form tumors with altered phospholipid metabolism and pH: A ^{31}P nuclear magnetic resonance study in vivo and in vitro. Magn Reson Med 41: 897-903, 1999.
47. Glunde K, Jacobs MA and Bhujwalla ZM: Choline metabolism in cancer: Implications for diagnosis and therapy. Expert Rev Mol Diagn 6: 821-829, 2006.
48. Ronen SM, Jackson LE, Beloueche M and Leach MO: Magnetic resonance detects changes in phosphocholine associated with *Ras* activation and inhibition in NIH 3T3 cells. Br J Cancer 84: 691-696, 2001.
49. Pollari S, Käkönen SM, Edgren H, Wolf M, Kohonen P, Sara H, Guise T, Nees M and Kallioniemi O: Enhanced serine production by bone metastatic breast cancer cells stimulates osteoclastogenesis. Breast Cancer Res Treat 125: 421-430, 2011.
50. Possemato R, Marks KM, Shaul YD, Pacold ME, Kim D, Birsoy K, Sethumadhavan S, Woo HK, Jang HG, Jha AK, *et al*: Functional genomics reveal that the serine synthesis pathway is essential in breast cancer. Nature 476: 346-350, 2011.
51. Locasale JW, Grassian AR, Melman T, Lyssiotis CA, Mattaini KR, Bass AJ, Heffron G, Metallo CM, Muranen T, Sharfi H, *et al*: Phosphoglycerate dehydrogenase diverts glycolytic flux and contributes to oncogenesis. Nat Genet 43: 869-874, 2011.
52. Sreekumar A, Poisson LM, Rajendiran TM, Khan AP, Cao Q, Yu J, Laxman B, Mehra R, Lonigro RJ, Li Y, *et al*: Metabolomic profiles delineate potential role for sarcosine in prostate cancer progression. Nature 457: 910-914, 2009.
53. Zhang WC, Shyh-Chang N, Yang H, Rai A, Umashankar S, Ma S, Soh BS, Sun LL, Tai BC, Nga ME, *et al*: Glycine decarboxylase activity drives non-small cell lung cancer tumor-initiating cells and tumorigenesis. Cell 148: 259-272, 2012.
54. Gmeiner WH, Hellmann GM and Shen P: Tissue-dependent and -independent gene expression changes in metastatic colon cancer. Oncol Rep 19: 245-251, 2008.
55. Shestov AA, Emir UE, Kumar A, Henry PG, Seaquist ER and Öz G: Simultaneous measurement of glucose transport and utilization in the human brain. Am J Physiol Endocrinol Metab 301: E1040-E1049, 2011.